PCCP

Accepted Manuscript

ROYAL SOCIETY OF CHEMISTRY

www.rsc.org/pccp

Stacking of purines in water: the role of dipolar interaction in caffeine

L. Tavagnacco[ab], S. Di Fonzo[a*], F. D'Amico[a], C. Masciovecchio[a], J. W. Brady[c], A. Cesàro[ab]

[a]*Elettra-Sincrotrone Trieste S.C.p.A., Strada Statale 14 Km 163.5, Area Science Park, I-34149 Trieste, Italy*

[b]*Lab. of Physical and Macromolecular Chemistry, Department of Chemical and Pharmaceutical Sciences, University of Trieste, via L. Giorgieri 1, 34127 Trieste, Italy*

[c]*Department of Food Science, Stocking Hall, Cornell University, Ithaca, New York, 14853, USA*

[*]*Corresponding author: Silvia di Fonzo*

Elettra-Sincrotrone Trieste S.C.p.A., Strada Statale 14 Km 163.5, Area Science Park,

I-34149 Trieste, Italy

Tel +39-040-375-8816

e-mail: silvia.difonzo@elettra.eu

Abstract

During the last decades it has been ascertained that base stacking is one of the major contributions stabilizing nucleic acid conformations. However, the understanding of the nature of the interactions involved in the stacking process remains under debate and it is a subject of theoretical and experimental studies. Structural similarity between purine bases (guanine and adenine) in DNA and the caffeine molecule makes caffeine an excellent model for the purine bases. The present study clearly shows that dipolar interactions play a fundamental role in determining stacking of purine molecules in solution. In order to reach this achievement, polarized ultraviolet Raman resonant scattering experiments have been carried out on caffeine aqueous solutions as a function of concentration and temperature. The investigation pointed out at the aggregation and solvation properties, particularly at elevated temperatures. Kubo-Anderson theory was used as a framework to investigate the non-coincidence effect (NCE) occurring in the totally symmetric breathing modes of the purine rings, and in the bending modes of the methyl groups of caffeine. The NCE concentration dependence shows that caffeine aggregation at 80 °C occurs by planar stacking of the hydrophobic faces. The data clearly indicate that dipolar interactions determine the reorientational motion of the molecules in solution and are the driving force for the stacking of caffeine. In parallel, the observed dephasing times imply a change in caffeine interactions as a function of temperature and concentration. A decrease, at low water content, of the dephasing time for the ring breathing vibration mode indicates that self-association alters the solvation structure that is detectable at low concentration. These results are in agreement with simulation predictions and serve as an important validation of the models used in those calculations.

Keywords: Caffeine, purine self-association, stacking and hydration, UV Raman resonant scattering, Raman non-coincidence effect, vibrational dephasing.

Introduction

Caffeine is a well-known constituent of widely consumed beverages such as coffee, tea and energy-drinks. It is a subject of interest for multiple reasons. While its food importance is obvious, caffeine is also important for its physiological effects and pharmaceutical properties.[1, 2] As a purine, its molecular structure resembles that of the DNA nucleotide bases,[3, 4] and its peculiar architecture makes the molecule largely hydrophobic in character, but soluble enough in water such that it can serve as a suitable model to test theories of hydrophobic hydration and aggregation.[5]

As with other purines, caffeine (1,3,7-trimethylxanthine) is characterized by a planar hydrophobic surface surrounded by both hydrophobic and hydrophilic functionalities, with a permanent electric dipole of ~3.6-3.7 D.[6] The hydrophilic groups, namely the hydrogen bonding acceptor groups O2, O6 and N9 and the hydrogen bonding-like donor group C8-H8, make the molecule slightly soluble in water. The molecular structure and the corresponding atomic labeling introduced in the present work are reported in Figure 1.

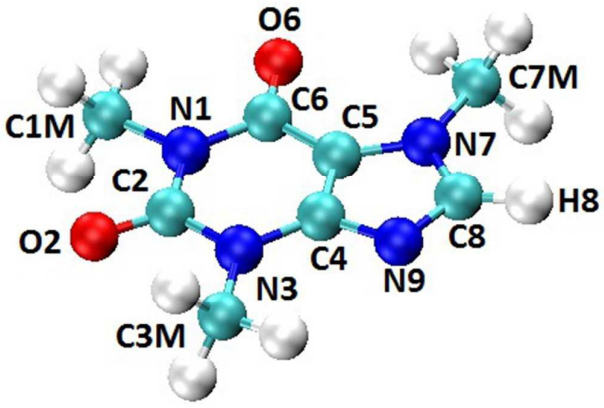

Figure 1. Caffeine molecular structure and atomic labeling adopted in the present work.

Experimental measurements, such as of the osmotic coefficient concentration dependence, have shown that caffeine molecules tend to aggregate at room temperature.[7] Molecular dynamics (MD) simulations have described these aggregates as stacks between the faces of the molecules.[5] This stacking aggregation is a type of hydrophobic association, resulting from the peculiar structuring imposed on solvent water molecules by the planar faces of the caffeine molecules, but unlike more typical hydrophobic associations, it is enthalpy-driven rather than entropy-driven.[7, 8] The aqueous solubility of caffeine increases at elevated temperatures, and MD simulations indicate that this may be due to a greater degree of stacking association. This behavior has important implications in several applications. Caffeine's low aqueous solubility limits its experimental characterization at ambient temperatures, but the strong enhancement of solubility at 80 °C has been exploited in a neutron scattering study,[9] and offers the opportunity of further experimental study.

During the last decades base stacking of nucleotides has been extensively studied by experimental and theoretical work. It has been established that stacking affinity and self-association of compounds like purine nucleobases, and not hydrogen bonding between the complementary strands of DNA, represent the major contributions to the free energy sustaining nucleic acid secondary structure. In particular, direct measurements by gel electrophoresis on DNA double helices have definitely established that the main contribution to the stability of DNA is stacking between adjacent bases.[10] Stacking is responsible for a large part of conformational variability, dynamics and stability of the DNA structure. Interactions involving base-stacking play an important role in the selective recognition of purine mononucleotides by macromolecules such as proteins and enzymes.[11] A full understanding of the self-assembly of a small but complex poly-functional molecule like caffeine will permit molecular engineering of specific molecular targets, by seeking an optimized therapy efficacious for transport of small drugs in the human body.[12]

Raman spectroscopy[13-17] is a valuable tool for extracting information about the inter-particle interaction potential of the molecular system under study using the shape and position of spectral bands at different temperature, density and molar fraction values.[18, 19] Specific information about the molecular aggregation states in systems with large dipole-dipole interactions can be determined by investigating the presence of the non-coincidence effect (NCE). This phenomenon is detected in normal modes with a strong infrared (IR) intensity in the gas phase and has been extensively observed in both Raman and IR strongly active bands, such as C=O,[20-28] SO,[29] NO_2 [30] and CN stretching.[31, 32] Because of its large dipole moment caffeine is expected to be a good candidate for a NCE investigation.

Although Raman spectroscopy has been widely used to investigate caffeine properties in the solid state,[33-35] and in solution with the Surface-enhanced Raman Scattering (SERS) modality,[36] the low solubility of caffeine in water is a limitation in obtaining high quality normal Raman spectra. Raman measurements carried out under UV resonance conditions may allow the enhancement of Raman features coming from collective vibrations of the aromatic rings. This occurs because of the π-π^* electronic transitions within the aromatic rings. These vibrations are expected to be more sensitive to the interactions between caffeine molecules, and therefore their enhancement will improve the interpretation of Raman spectra with an appreciable signal-to noise ratio. In fact, by taking advantage of the high sensitivity of the resonance technique it is possible to study solutions even at low caffeine concentration (such as 1 caffeine molecule in about 25000 water molecules).

MD simulations of aqueous systems potentially can provide complete detail about solution structure and organization, but the results of such simulations are only useful if the various force fields and approximations employed accurately represent the physical system being studied. This limitation is particularly true for systems containing less fully characterized solutes like caffeine, or at elevated temperatures far from the conditions for

which the water models were developed. There is thus a critical need for experimental methods that can probe the organization of such solutions, as a demanding test of simulation results. With these possibilities in mind, a Raman resonance scattering investigation of caffeine aqueous solutions as a function of concentration and temperature has been carried out, with the objective of investigating its hydration and aggregation properties, complementing previous MD results.[5, 9] In particular, by combining results from quantum chemistry computations and resonance Raman experiments, some light could be shed on the role played by the hydrophobic and hydrophilic interactions, including dipolar correlations, in caffeine under a wide range of concentrations. The results show that caffeine molecules were found to be clustered by planar stacking between the hydrophobic faces also in solution at 80 °C and that the interactions of this specific molecule at elevated temperatures not only have important biotechnological applications but also serve as a model for purine stacking in nucleic acids under similar conditions, as, for example in extremophiles.

Methods

Quantum chemical computations

In order to simulate the Raman spectra, the ground state molecular structure of caffeine was optimized using second order Møller-Plesset (MP2) perturbation theory[37] with the Gaussian 09 software package.[38] The geometry optimization was carried out using the 6-311++G(d,p) basis set. Harmonic frequencies were calculated with the density functional theory employing B3LYP exchange-correlation functional and the 6-311++G(2d,2p) basis set, as this was found to be the best procedure in the work of Srivastava and Singh.[39] We have been encouraged by the method provided by these authors, showing correspondence without scaling between calculated and experimental data up to ca. 2000 cm^{-1}. However, two slightly different sets of optimized geometrical parameters were used as input in this work and in the

Srivastava and Singh work. It should be noted that even these small differences of coordinates (of 0.005 Å) can produce spectral differences,[39] which, nonetheless, are not matter of discussion in this paper. Only real harmonic wave numbers were produced. Calculated normal modes and corresponding assignments are reported in the Electronic Supplementary Information (ESI) (Table S1). No scaling factor was applied to the calculated vibrational modes. The caffeine structure was optimized without an explicit treatment of solvent environment. It seems likely that the principal perturbation from interaction with solvent would be through hydrogen bonding to the carbonyl groups, the nitrogen atom N9 and possibly the anomalous H8 proton. However, such interactions take place primarily in the plane of the caffeine molecule and simulations have shown that these are not affected from stacking.[5, 9]

Following a Reviewer's suggestion, harmonic frequencies were also calculated for caffeine dimers. Two different configurations were considered: the parallel dimer having stacked molecules with dipole moment vectors aligned and pointing the same direction and the antiparallel dimer having stacked caffeine molecules with dipole moment vectors aligned and pointing opposite directions (see Figure S4 in the ESI). Geometry was optimized with the density functional theory employing B3LYP exchange-correlation functional and the 6-311G(d,p) basis set. Harmonic frequencies were calculated employing B3LYP and 6-311G(2d,2p) basis set.

UV Raman scattering measurements and data analysis

Ultraviolet (UV) resonance Raman scattering experiments were carried out at the BL10.2–IUVS beamline at the Elettra Synchrotron Laboratory in Trieste.[40] The isotropic and anisotropic Raman spectra (see ESI) were acquired at wavelength λ=266 nm at different

temperatures, from 300K to 353 K. The experimental resolution was set to 5 cm^{-1}. Caffeine aqueous solutions (Sigma-Aldrich, purity by HPLC > 99.0 %) were contained in a UV-grade quartz cell. All experimental data in the region at about 1550 cm-1 are affected by an erroneous peak of about 10 cm-1 FWHM. The feature is an artifact and arises from a laser satellite. We have deleted the points in this region, since the peak appears also in the empty cell.

Data were analyzed using the Kubo Anderson framework (KAF).[41, 42] This model allows the determination of the vibrational dephasing relaxation time, τ_{vibr}, and the reorientational relaxation time τ_{reor} (see ESI). The non coincidence effect, NCE, was also studied as a function of the temperature and the concentration.

Results and Discussion

Figure 2 shows the comparison between one representative experimental Raman profile for a solution of caffeine and the theoretical Raman intensity and activity obtained by quantum chemical computation in vacuum on the caffeine molecule. Small differences appear in the experimental resonance Raman spectra in comparison with the normal Raman spectra (table S1 in ESI). The band assignment has been made by comparison of wavenumbers and relative intensities for the theoretical and experimental profiles, the resulting peak assignment being in agreement with the work of Srivastava and Singh[39]. The experimental symmetric band centered at about 1290 cm^{-1}, labelled as ν_{rings}, is mainly associated with stretching vibration modes of the C-C and C-N atoms in both rings of caffeine plus a minor contribution due to the stretching of the N3-C3M in the pyrimidine ring. The main axis of the scattering vector for the transition dipole is oriented, in the purine plane, perpendicularly to the permanent dipole of the molecule, as indicated in the schematic picture of this vibration at the

top of Figure 2a. As will be discussed later, ν_{rings} is important in monitoring molecular aggregation.

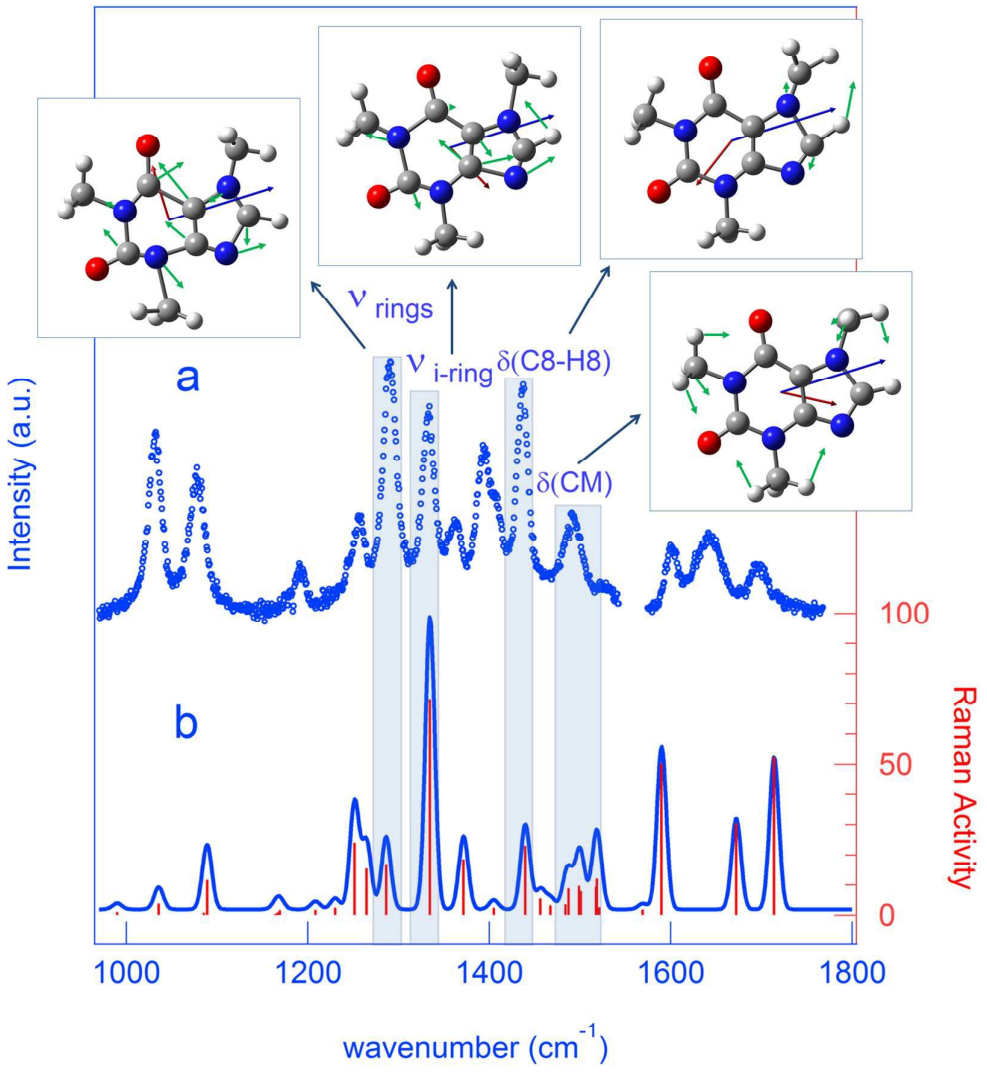

Figure 2. a) Experimental Raman spectra for caffeine solution at 1m and 353 K (data at about 1550 cm^{-1} are affected by an experimental laser satellite artifact and therefore are omitted, see Methods). b) Simulated Raman activity (red bars) and intensity profile (blue curve). The latter has been obtained by convolution with a Gaussian function of 5 cm^{-1} width. At the top a schematic picture of the indicated vibration lines of caffeine molecule. Permanent dipole moment vectors (light-blue arrow), transition dipole moment vectors (red arrow), and displacement vectors (green) for the corresponding vibration are also indicated.

The very intense vibrational peak found at about 1335 cm^{-1} in the experimental spectrum, labelled as $\nu_{i\text{-}ring}$ is associated with the stretching of the imidazole ring, in accordance with previous work.[39]

Two bands provide dynamic information on the hydrophilic or hydrophobic character of the caffeine molecule, specifically, the intense and narrow band centered at about 1437 cm^{-1} in the experimental spectra, labelled as $\delta(C8-H8)$, is associated with the bending of the indicated atoms in the imidazole group. This site is highly hydrophilic, as shown in previous investigations realized on caffeine and purine molecules,[5, 43] and favors the formation of anomalous hydrogen bonds with water in the solid state.[44, 45] The broad band centered at about 1492 cm^{-1}, labelled as $\delta(CM)$, is associated with several vibration lines, each of them involving, as a major component, the symmetric and asymmetric bending modes of the hydrophobic methyl groups of caffeine.

As shown in the simulated spectra reported in Figure 2b, $\nu_{i\text{-}ring}$ has by far the highest Raman activity. The significant enhancement observed for the experimental intensity of ν_{rings}, $\delta(C8-H8)$ and $\delta(CM)$ Raman bands follows because of the electronic $\pi \rightarrow \pi^*$ transition occurring at about 273 nm.[46] This transition is highly delocalized and involves the entire molecule, leading to a quite unselective peak enhancement, in addition to a significant reduction of the fluorescence background, as compared to the background obtained with an excitation source in the visible. This enhancement of the Raman cross section allows the spectral analysis of extremely diluted samples, such as 0.0022 m (See Figure S1, ESI).

As already mentioned, a quantitative description of the concentration dependence of the isotropic Raman profiles can be achieved by applying the fitting procedure based on the KAF model,[41] already used for other aqueous solutions.[47, 48] This methodology was adopted

here to analyze the Raman spectrum in the whole experimentally measured range to ensure the maximum likelihood of the results. Figure 3 reports an example of the fitting procedure.

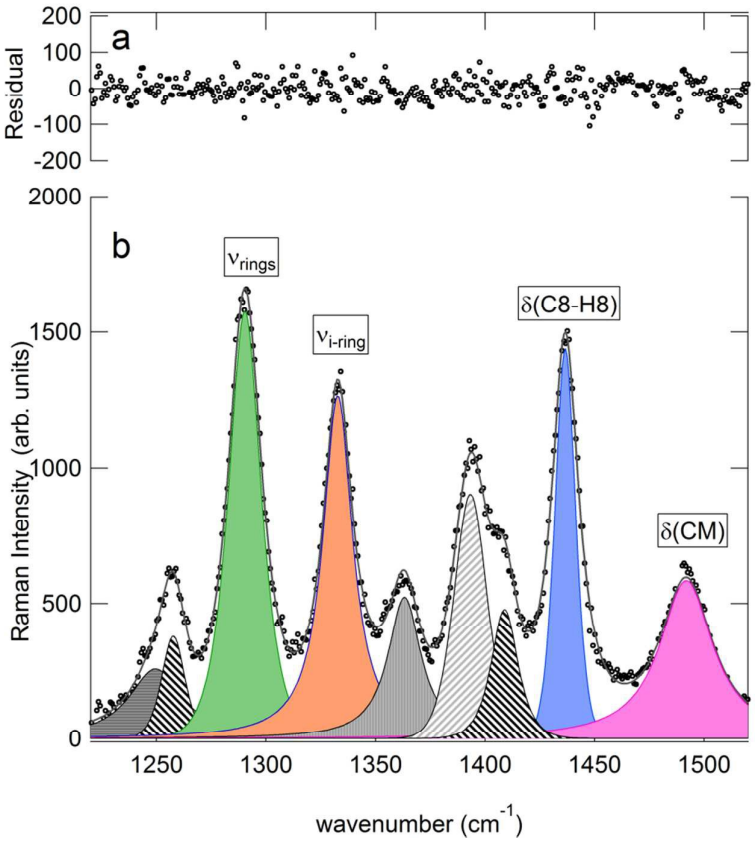

Figure 3. Representative example (T=353 K and 1 m concentration) of the fitting procedure for the isotropic Raman profiles of caffeine solutions in the spectral range 1200-1500 cm^{-1} a) fit residuals; b) peak deconvolution and curve fit.

In the present work the analysis has focused on the vibrational normal modes that were expected to be more affected by the hydration and aggregation processes.[5] Figure 4 reports some representative examples of the concentration dependence of the isotropic peak positions exhibited by the vibrational normal mode associated with the in-plane bending of $C8-H8$ and with the bending of the methyl groups. Upon dilution of caffeine, up to about 0.1 m, a shift can be seen in the peak positions towards higher wavenumbers. Below this value of caffeine concentration the blue shift disappears and the slope in the logarithmic horizontal scale flattens. This effect is reproduced by all the bands with the exception of those associated with the stretching of the carbonyl atoms that shows the opposite behavior, as confirmed by the studies already reported in literature[49] (see Figure S2 in the ESI). The detected concentration dependence can be explained by taking into account that, as the water content increases, caffeine molecule clusters progressively break up into individual molecules. Van der Waals interactions between adjacent caffeine molecules become weaker, with the result that the vibrational bands, and especially that of the hydrophobic methyl groups, are enhanced in intensity and a blue-shift is detected. The formation of hydrogen bonds with the atoms of the rings mitigates this effect, leading to a slightly smaller blue-shift, as can be seen for the $C8-H8$ bending.

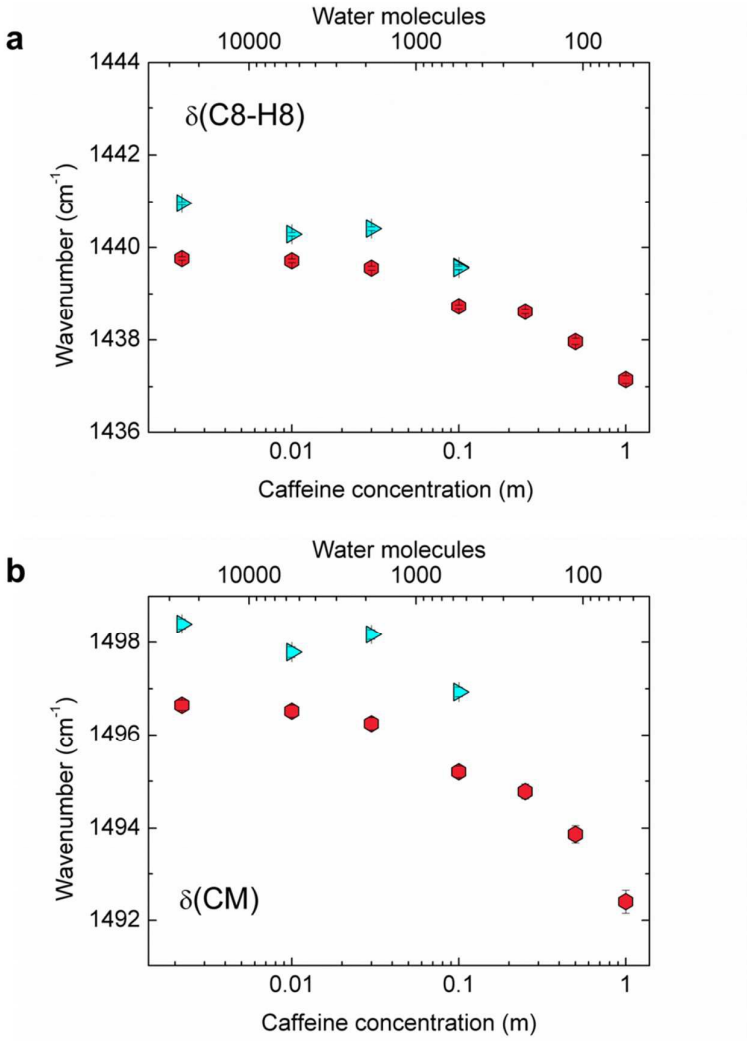

Figure 4. Concentration dependence of the isotropic peak position for the normal modes associated to the bending of $C8-H8$ (a) and the bending of the methyl groups (b). Results obtained at 300K are displayed in light blue, whereas those obtained at 353K are represented in red.

The KAF model predicts that when the modulation of the probe molecule is fast compared to molecular perturbations of the system in which it is embedded, the band-shape reduces to a Lorentzian function and both the vibrational dephasing relaxation time and the reorientational relaxation time of the entire molecule can be calculated following equations 5a and 5b in the ESI. The present study investigates two vibrational normal modes that satisfy

this condition: the stretching of the imidazole ring and the bending of the methyl groups. In Figure 5 the concentration dependence and the temperature dependence of the vibrational dephasing for the normal mode associated with the stretching of the imidazole ring are reported. Both at room temperature and at 353 K the dephasing time exhibits a decrease as a function of the caffeine content. Because of the caffeine solubility limit, a narrow range of concentrations could be investigated at 300 K. At constant 0.1 m caffeine concentration the vibrational dephasing becomes shorter upon increasing the temperature.

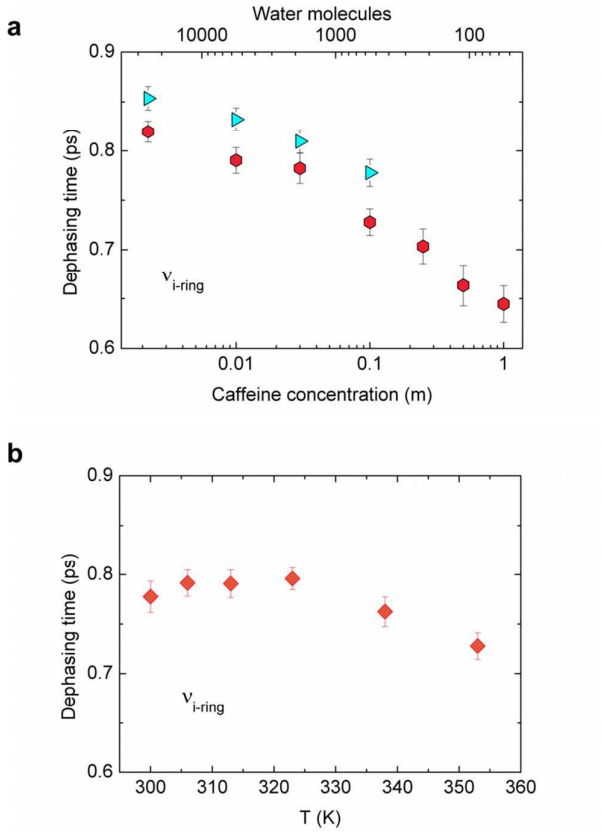

Figure 5. a) Concentration dependence of the vibrational dephasing calculated for the vibrational normal mode involving the caffeine imidazole ring atoms measured at 300K (light-blue triangles) and 353K (red circles). b) Temperature dependence of the vibrational dephasing calculated for the vibrational normal mode involving the caffeine imidazole ring atoms measured for a 0.1m caffeine aqueous solution.

These characteristic features reflect the behavior of the caffeine environment. In particular, at low concentration, where the extent of the caffeine self-association is weak, the dynamics is dominated by the solvent structuring around the caffeine molecules. These neighboring water molecules are strongly structured.[5] Upon increasing the caffeine concentration, and thus necessarily the temperature, the vibrational dephasing becomes shorter because the strong caffeine self-association results in the release of the water molecules originally structured around the isolated caffeine functionalities.

Figure 6 shows the comparison between the vibrational dephasing calculated for the imidazole ring stretching and the methyl group atom bending. The effect of the caffeine concentration is stronger for the vibrational normal mode associated with the caffeine ring atoms. As will be illustrated in the next paragraph, this effect is a result of caffeine self-association, which involves a minor variation of the molecular environment of the caffeine methyl groups because self-aggregation mainly involves a stacking between hydrophobic rings.

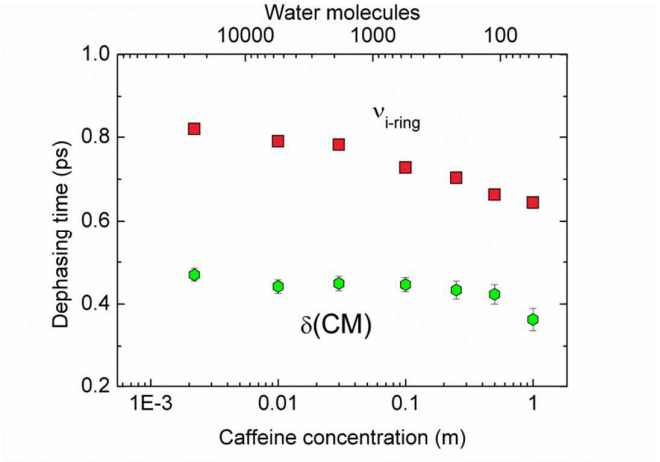

Figure 6. Concentration dependence of the vibrational dephasing calculated for the vibrational normal mode involving the caffeine side methyl group atoms (green circles) compared to that calculated for the imidazole ring stretching (red squares) measured at 353K.

The NCE concentration dependence[50], at room and high temperature, for the totally symmetric breathing modes of the purine rings, ν_{rings}, and for the bending modes of methyl groups of caffeine, $\delta(CM)$, is reported in Figure 7 (see Figure S3 in ESI for corresponding isotropic and anisotropic spectra). Although an increase in temperature is generally expected to reduce the magnitude of the NCE,[50] a strong positive effect was observed, suggesting the presence of solute interactions in solution.

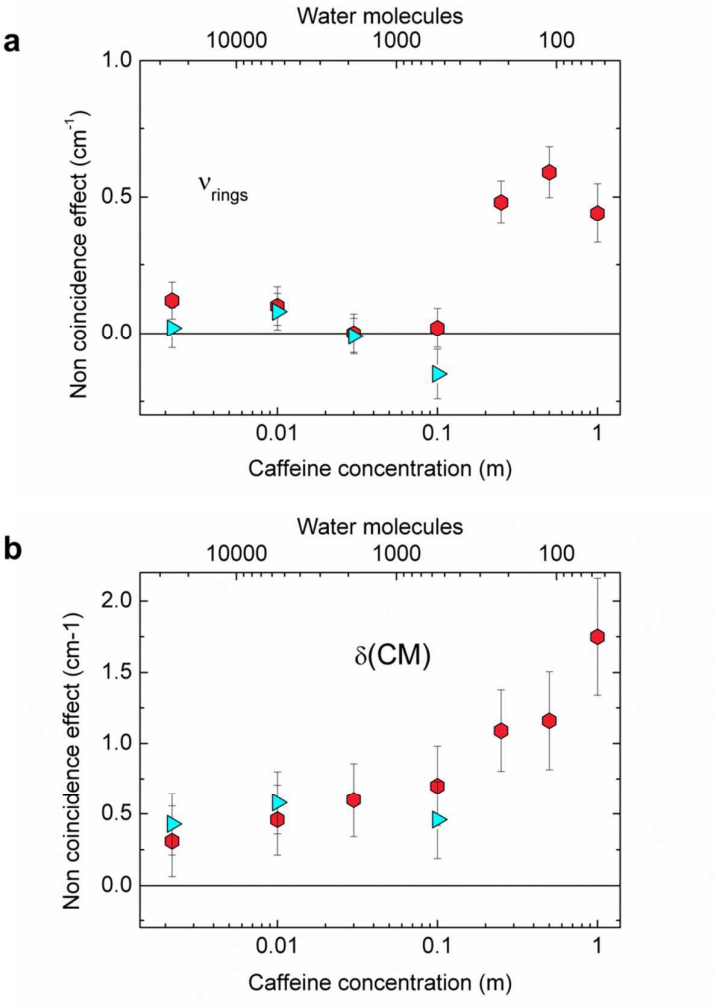

Figure 7. Non-coincidence effect concentration dependence for the vibrational normal mode associated to the C-C C-N stretching in both rings (a) and for the symmetric bending modes of the hydrophobic methyl groups (b). Results obtained at 300K are displayed in light blue, whereas those obtained at 353K are represented in red.

Figure 7 shows that in the case of the vibrational normal modes involving the caffeine ring atoms the NCE increases with the caffeine concentration up to a plateau, whereas the NCE associated with the bending of the caffeine methyl groups increases monotonically as a function of the concentration. At high water content, both at 300K and 353K, no significant NCE effect is detectable for the vibrational modes involving the ring or the side atom movements.

This is the first report of a detected NCE in the totally symmetric breathing modes of the purine rings and in the bending modes of methyl groups of caffeine. A number of theoretical models have been proposed to interpret this effect.[51, 52,53] All models suggested the presence of a certain degree of reorientational order in the liquid, the sign of $\Delta\nu_{NCE}$ being determined by the angle between the main axes of the scattering tensors of interacting vibrators.[54]

The most extensive theoretical treatment of non-coincidence splitting in the Raman spectra of binary mixtures has been developed by Logan and coworkers.[55,53] According to Logan, for a given temperature T, the concentration dependence of the difference in wavenumber between the anisotropic and isotropic component of the Raman spectra can be obtained by the following approximate expression:

$$\Delta\omega(\phi_{caff}) = \frac{\phi_{caff}\,\xi_0}{c\,t_D}\frac{1+\frac{5}{4}y_0(\phi_{caff})}{\left[1+\frac{5}{2}y_0\,(\phi_{caff})\right]^2} \qquad [1]$$

where

$$y_0(\phi_{caff}) \approx \xi_0\ \left[\phi_{caff} + \left(\frac{\mu_w}{\mu_{caff}}\right)^2 \frac{1-\phi_{caff}}{R}\right] \qquad [2]$$

and

$$\xi_0 = \frac{\mu_{caff}\,\varrho_{caff}}{72K_B T\epsilon_0} \qquad [3]$$

In the above expressions the concentration is expressed in terms of the caffeine volume fraction, ϕ_{caff}. The values for the number density and the molar volume for pure caffeine have been taken from the data reported in the literature for the anhydrous crystalline form of caffeine[56] ρ_{caff}= 4.59X10^{21} cm^{-3} and V_{caff}=131 cm^3. The permanent dipole of caffeine[6] and water are μ_{caff}= 3.7 D and μ_w= 1.847 D, respectively. The parameter t_D has the dimensions of time and depends only on the molecular properties and on the transition dipole of the vibrational mode, not on thermodynamics parameters.[53]

Assuming that ρ_{caff} and V_{caff} do not vary significantly with temperature in the considered temperature range, as the investigated temperatures are much lower than the caffeine melting point, the calculated ratio between the molar volumes $R=V_w/V_{caff}$ is therefore R=0.1374 at T 300 K and R= 0.1414 at T=353 K. In the present case the calculated values for ξ_0 are 0.265 and 0.225 for T=300 and T= 353 K, respectively.

The relative non coincidence splitting, hence independent of the transition dipole moment of the specific vibration, predicted from the equations above is indicated in Figure 8 together with the NCE associated with the bending of the caffeine methyl groups and the NCE associated with the C-C and C-N stretching in both caffeine rings for the indicated temperatures. The concentration scale has been expressed in caffeine volume fraction.

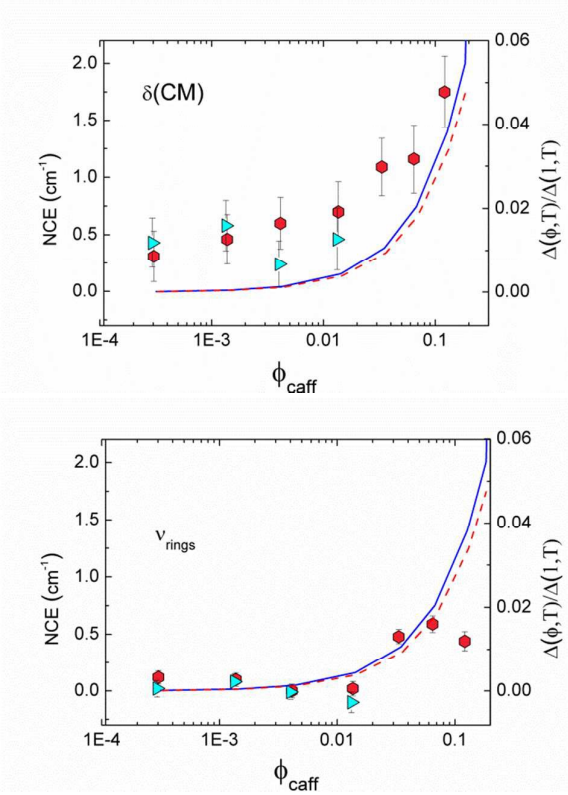

Figure 8 (Left) Concentration dependence of the experimental non-coincidence effect for the bending of the methyl groups (dots). (Right) Concentration dependence of the experimental non-coincidence effect for the vibrational normal mode associated to the C-C C-N stretching in both rings (dots). Results obtained at 300K are displayed in light blue, whereas those obtained at 353K are represented in red. In both graphs the lines represent the relative NCE obtained by applying the Logan theory (see text).

The model and the experimental data are approximately in agreement at low caffeine concentration where, both at 300K and 353K, the NCE is predicted to be negligible. In the case of the experimental data concerning the bending of the methyl groups, a rigid shift towards higher NCE values can be seen that can be attributed to the asymmetry of the peak, which also results in the higher uncertainty of the peak position. Increasing the caffeine content, the model produces a monotonically increasing function that is weakly dependent on the temperature. This regime of concentration cannot be experimentally reached at room temperature, but only at 353K. As shown in Figure 8, the experimental trend of the NCE

concentration dependence at 353K in the case of the methyl group bending is similar to that predicted by the theory, whereas for the stretching of atoms in both caffeine rings it is completely different.

Caffeine is known to self-associate in aqueous solution, as shown by previous experimental studies on concentration dependence of the osmotic coefficients and density data.[7] Molecular dynamics simulations carried out at 298 K [5] and at 353 K [9] showed that, at the microscopic level, this aggregation can be described as a stacking like coins between caffeine planar faces. As the general red-shift detected with caffeine concentration at both 300K and 353K validates the formation of aggregates between the caffeine molecules at lower water content, information on the local organization can be extrapolated through the observation of the Raman non-coincidence effect. An important feature of the investigated vibrational normal modes is that the permanent dipole moment and the transition dipole moment are oriented in the plane of the caffeine molecule (Figure 2 top). In addition, only in the case of the purine ring stretching, the transition dipole moment vector is perpendicular to the caffeine permanent dipole moment. According to the transition dipole-transition dipole mechanism of vibrational coupling[54], the NCE depends on the mutual orientation of interacting dipoles and on the derivative of the dipole moment with respect to the vibrational coordinate of the interacting vibrators. The effect is the integral function of the dot product of the dipole moment vectors. Thus, if all molecular orientations have the same probability, the resulting effect is null.

In the presence of permanent dipole moment vectors oriented in the plane of the caffeine molecules, the positive NCE indicates that the geometry of the interacting molecules can only be a stacking between the caffeine faces. In addition, in order to detect a NCE, a necessary, even if not sufficient, condition is that adjacent caffeine molecules orient themselves with a preferred (parallel or anti-parallel) orientation of the dipole moments,

while a perpendicular orientation of the nearest-neighbor molecule will give no contribution at all.

This NCE concentration dependence suggests that the formation of aggregates reaches a regime where almost no individual caffeine monomers are present. Indeed, at high concentration no further increase of the NCE effect is detectable for the movements of the ring atoms because they are already influenced by the presence of adjacent caffeine molecules. Conversely, the vibrational normal modes of the caffeine atoms located in the side arms are affected by the size of the caffeine clusters and by the formation of side branches. The comparison of the experimental data with the Logan model confirms our hypothesis that the saturation of the NCE signal from the ring vibration is due to its short-range sensitivity as compared to the vibration of the methyl groups.

An estimate of the NCE associated to the experimentally studied normal modes ν_{rings} and δ_{CM} can be obtained from the calculation of the isotropic and anisotropic Raman activity of simulated caffeine dimers (see Table S3 in the ESI). Although coupled modes cannot be separated into pure isotropic and anisotropic modes, the corresponding isotropic and anisotropic Raman activities indicate that in both the investigated configurations (parallel and antiparallel stacking) the associated NCE is positive. In addition, in agreement with the magnitude of the NCE measured experimentally, the frequency splitting of the bending of the methyl groups δ_{CM} is higher than that of the breathing mode of the purine ring ν_{rings}.

This experimental characterization of caffeine aqueous solution at 353 K validates the complementary MD simulations and Empirical Potential Structure Refinement (EPSR) simulations of neutron scattering data,[9] carried out at the same temperature, that report a tendency of the system to form aggregates. Both the MD and EPSR simulations are consistent with an extensive aggregation of caffeine also at 353 K.

Figure 9 reports the reorientational relaxation times calculated for the imidazole ring stretching as a function of the caffeine concentration and the temperature at a concentration of 0.1 m of caffeine. The values of the reorientational relaxation time confirm *a posteriori* that the vibrational and rotational processes are decoupled. The reorientational relaxation time increases exponentially with the caffeine concentration as expected from the formation of caffeine aggregates with hampered freedom.

Assuming an Arrhenius temperature dependence of the reorientational relaxation time (see ESI, Figure S5), the estimated activation energy E_a gives a value of 2 kcal mol^{-1} (±0.5 kcal mol^{-1}). This assumption should take care of the fact that changes in the distribution of relaxation times with temperature are expected, since the population of stacked species decreases upon increasing the temperature. Nonetheless, the approximate value of the activation energy is conceivable and is slightly smaller than the experimentally measured association energy (-3.4 kcal mol^{-1} at 298 K[7]) indicating the strong contribution of the dipolar interaction to the orientation and stability of the stacked species. A similar value of the energy can be extracted from MD simulation studies for the energy barrier of the dependence of population of caffeine stacks as a function of the orientation of caffeine planes (1.2 kcal/mol at 298 K)[5].

A recent review of the nature and magnitude of base stacking in nucleic acids points out the difficulty of avoiding overestimation or underestimation of intrinsic stacking interaction in computational approaches, foreseeing the need for cooperation between theory and experiment for computational insights into different types of experiments.[57]

Finally, it is worth mentioning that a correlation can be found between the reorientational time calculated for the vibrational normal mode involving the caffeine imidazole ring and the non-coincidence effect calculated for the vibrational normal mode

involving the caffeine methyl groups atoms (See Figure S6, ESI). It can be deduced from this observation that the two phenomena both can be attributed to the caffeine self-association.

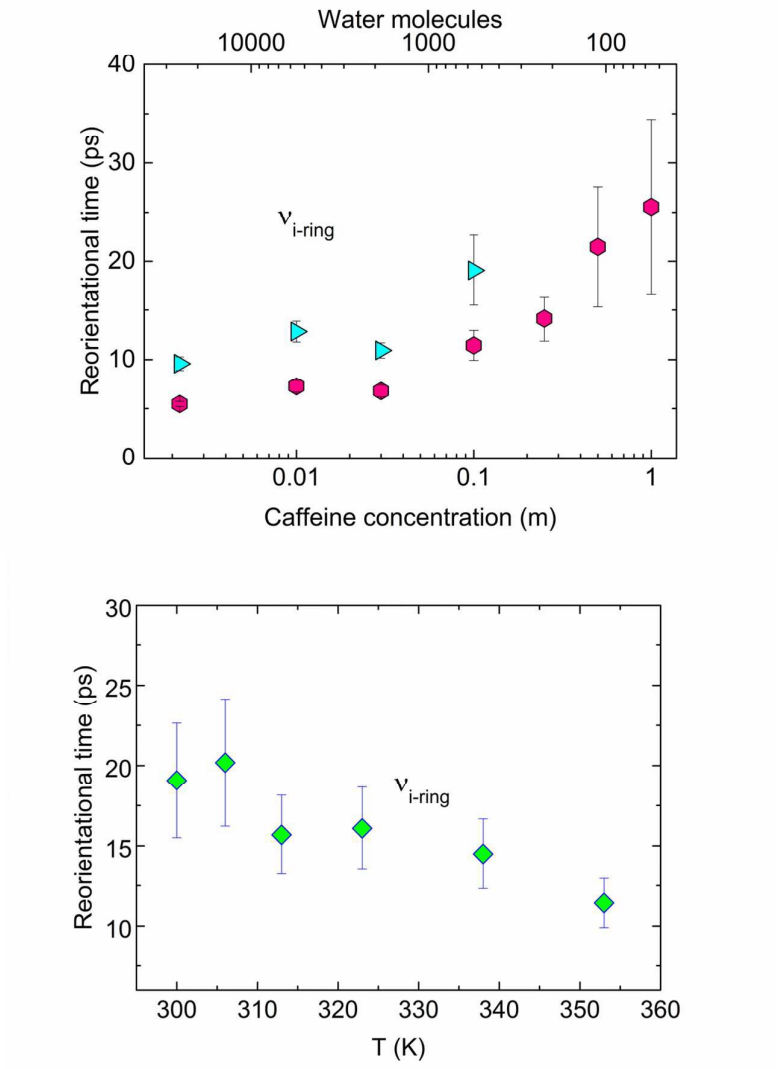

Figure 9 On the top, concentration dependence of the reorientational relaxation time calculated for the vibrational normal mode involving the caffeine imidazole ring atoms measured at 300K (light-blue triangles) and 353 K (red squares). At the bottom, temperature dependence of the reorientational relaxation time calculated for the vibrational normal mode involving the caffeine imidazole ring atoms measured on a 0.1m caffeine aqueous solution.

Summary and Conclusions

The present UV resonance Raman scattering study shows that caffeine molecules tend to form aggregates in aqueous solution at 80 °C by the formation of stacks between the hydrophobic faces of the molecules. For the first time the NCE was found to occur in the totally symmetric breathing modes of the purine rings and in the bending modes of the methyl groups of caffeine. The measured non-coincidence effect suggests that dipolar interactions play an important role in the formation of caffeine aggregates at high temperature. The achievement of this information and the study of systems at low caffeine content, such as 1 caffeine molecule in about 25000 water molecules, were possible only by taking advantage of the high sensitivity of the resonance technique. These findings are in agreement with previous computational investigations at 80 °C.[9] In addition, it has been found that at 80 °C the caffeine molecules in the aggregates tend to organize so as to avoid a perpendicular orientation of the permanent dipole moment vectors of adjacent molecules. This observation is in agreement with previous results obtained through MD simulations at room temperature. There are few experimental methods that can characterize such solution behavior at this level of detail, and the present results thus represent an important test of the validity of simulation results. Osmotic measurements of caffeine solutions can only confirm association, and not provide structural details. The more detailed comparison possible using the present NCE results is vital before accepting simulation details that cannot be otherwise experimentally confirmed. Small Angle Neutron Scattering experiments have been carried out to provide complementary information on the size and shape of the caffeine clusters detected in solution (to be published).

The Raman non-coincidence effect is a powerful tool for acquiring information on molecular orientation at the microscopic level. With Raman scattering experiments we were able to characterize the local organization of the caffeine molecules in solution. Having

established the strong potential of this approach and given that the detected base pairing is recognized to be one of the major contributions to the DNA double helix stability, this technique shows promise for being extended to characterize the conformational properties of more complex DNA structures.

Acknowledgements

We thank Alessandro Gessini, BL10.2–IUVS Beamline Operation Manager, for technical help during the measurements. We thank Daniele Toffoli for helpful discussions.

Support for computational work by CINECA ISCRA grants (Bologna, Italy) is gratefully acknowledged.

References

1. T. Ranheim and B. Halvorsen, *Molecular Nutrition & Food Research*, 2005, **49**, 274-284.
2. R. M. van Dam, *Applied Physiology, Nutrition, and Metabolism*, 2008, **33**, 1269-1283.
3. M. T. Record, S. J. Mazur, P. Melancon, J. H. Roe, S. L. Shaner and L. Unger, *Annual Review of Biochemistry*, 1981, **50**, 997-1024.
4. M. Kabelac and P. Hobza, *Physical Chemistry Chemical Physics*, 2007, **9**, 903-917.
5. L. Tavagnacco, U. Schnupf, P. E. Mason, M.-L. Saboungi, A. Cesàro and J. W. Brady, *The Journal of Physical Chemistry B*, 2011, **115**, 10957-10966.
6. C. Párkányi, C. Boniface, J.-J. Aaron, M. Bulaceanu-MacNair and M. Dakkouri, *Collect. Czech. Chem. Commun.*, 2002, **67**, 1109–1124.
7. A. Cesàro, E. Russo and V. Crescenzi, *The Journal of Physical Chemistry*, 1976, **80**, 335-339.
8. P. R. Stoesser and S. J. Gill, *The Journal of Physical Chemistry*, 1967, **71**, 564-567.
9. L. Tavagnacco, J. W. Brady, F. Bruni, S. Callear, M. A. Ricci, M. L. Saboungi and A. Cesàro, *The Journal of Physical Chemistry B*, 2015, DOI: 10.1021/acs.jpcb.5b09204.
10. P. Yakovchuk, E. Protozanova and M. D. Frank-Kamenetskii, *Nucleic Acids Research*, 2006, **34**, 564-574.
11. K. J. Neurohr and H. H. Mantsch, *Canadian Journal of Chemistry*, 1979, **57**, 1986-1994.
12. D. Davies, D. Veselkov, L. Djimant and A. Veselkov, *Eur Biophys J*, 2001, **30**, 354-366.
13. N. G. Bakhshiev, *Spectroscopy of Intermolecular Interactions*, Nauka, Leningrad, 1972.
14. J. H. Campbell, J. F. Fisher and J. Jonas, *The Journal of Chemical Physics*, 1974, **61**, 346-360.
15. W. G. Rothschild, *Dynamics of Molecular Liquids*, Wiley, New York, 1984.
16. P. Hildebrandt, M. Tsuboi and T. G. Spiro, *The Journal of Physical Chemistry*, 1990, **94**, 2274-2279.
17. W. K. Bischel and M. J. Dyer, *Physical Review A*, 1986, **33**, 3113-3123.
18. S. A. Kirillov, *Chemical Physics Letters*, 1999, **303**, 37-42.
19. N. Nishi, T. Nakabayashi and K. Kosugi, *The Journal of Physical Chemistry A*, 1999, **103**, 10851-10858.
20. M. G. Giorgini, M. Musso, A. Asenbaum and G. Döge, *Molecular Physics*, 2000, **98**, 783-791.
21. M. Musso, M. G. Giorgini, G. D. Asenbaum and A, *Molecular Physics*, 1997, **92**, 97-104.
22. D. H. Torii M. Musso M. G. Giorgini G, *Molecular Physics*, 1998, **94**, 821-828.
23. V. Shelley and J. Yarwood, *Molecular Physics*, 1991, **72**, 1407-1423.
24. T. F. Sun, J. B. Chan, S. L. Wallen and J. Jonas, *The Journal of Chemical Physics*, 1991, **94**, 7486-7493.
25. H. D. Thomas and J. Jonas, *The Journal of Chemical Physics*, 1989, **90**, 4144-4149.
26. M. G. Giorgini, G. Fini and P. Mirone, *The Journal of Chemical Physics*, 1983, **79**, 639-643.
27. V. L. Slager, H.-C. Chang, Y. J. Kim and J. Jonas, *The Journal of Physical Chemistry B*, 1997, **101**, 9774-9781.
28. M. S. Bradley and J. H. Krech, *The Journal of Physical Chemistry*, 1993, **97**, 575-580.

29. C. Czeslik, Y. J. Kim and J. Jonas, *The Journal of Chemical Physics*, 1999, **111**, 9739-9742.
30. A. Morresi, L. Mariani, R. S. Cataliotti, M. G. Giorgini, M. R. Distefano and G. Giaquinta, *Journal of Molecular Structure*, 1993, **293**, 227-230.
31. H. Torii and M. Tasumi, *The Journal of Chemical Physics*, 1993, **99**, 8459-8465.
32. A. Morresi, M. Paolantoni, P. Sassi, R. S. Cataliotti and G. Paliani, *Journal of Physics: Condensed Matter*, 2000, **12**, 3631.
33. J. D. Taeye and T. Z. Huyskens, *Spectroscopy Letters*, 1986, **19**, 299-310.
34. A. Hédoux, L. Paccou, P. Derollez and Y. Guinet, *International Journal of Pharmaceutics*, 2015, **486**, 331-338.
35. H. G. M. Edwards, T. Munshi and M. Anstis, *Spectrochimica Acta Part A: Molecular and Biomolecular Spectroscopy*, 2005, **61**, 1453-1459.
36. I. Pavel, A. Szeghalmi, D. Moigno, S. Cîntă and W. Kiefer, *Biopolymers*, 2003, **72**, 25-37.
37. C. Møller and M. S. Plesset, *Physical Review*, 1934, **46**, 618-622.
38. M. J. Frisch, G. W. Trucks, H. B. Schlegel, G. E. Scuseria, M. A. Robb, J. R. Cheeseman, G. Scalmani, V. Barone, B. Mennucci, G. A. Petersson, H. Nakatsuji, M. Caricato, X. Li, H. P. Hratchian, A. F. Izmaylov, J. Bloino, G. Zheng, J. L. Sonnenberg, M. Hada, M. Ehara, K. Toyota, R. Fukuda, J. Hasegawa, M. Ishida, T. Nakajima, Y. Honda, O. Kitao, H. Nakai, T. Vreven, J. A. Montgomery, J. E. Peralta, F. Ogliaro, M. Bearpark, J. J. Heyd, E. Brothers, K. N. Kudin, V. N. Staroverov, R. Kobayashi, J. Normand, K. Raghavachari, A. Rendell, J. C. Burant, S. S. Iyengar, J. Tomasi, M. Cossi, N. Rega, J. M. Millam, M. Klene, J. E. Knox, J. B. Cross, V. Bakken, C. Adamo, J. Jaramillo, R. Gomperts, R. E. Stratmann, O. Yazyev, A. J. Austin, R. Cammi, C. Pomelli, J. W. Ochterski, R. L. Martin, K. Morokuma, V. G. Zakrzewski, G. A. Voth, P. Salvador, J. J. Dannenberg, S. Dapprich, A. D. Daniels, Farkas, J. B. Foresman, J. V. Ortiz, J. Cioslowski and D. J. Fox, *Journal*, 2009, DOI: citeulike-article-id:9096580.
39. S. K. Srivastava and V. B. Singh, *Spectrochimica Acta Part A: Molecular and Biomolecular Spectroscopy*, 2013, **115**, 45-50.
40. F. D'Amico, M. Saito, F. Bencivenga, M. Marsi, A. Gessini, G. Camisasca, E. Principi, R. Cucini, S. Di Fonzo, A. Battistoni, E. Giangrisostomi and C. Masciovecchio, *Nuclear Instruments and Methods in Physics Research Section A: Accelerators, Spectrometers, Detectors and Associated Equipment*, 2013, **703**, 33-37.
41. L. Mariani, A. Morresi, R. S. Cataliotti and M. G. Giorgini, *The Journal of Chemical Physics*, 1996, **104**, 914-922.
42. W. G. Rothschild, *The Journal of Chemical Physics*, 1976, **65**, 455-462.
43. M.-k. Teng, N. Usman, C. A. Frederick and A. H.-J. Wang, *Nucleic Acids Research*, 1988, **16**, 2671-2690.
44. D. Sutor, *Acta Crystallographica*, 1958, **11**, 453-458.
45. G. D. Enright, V. V. Terskikh, D. H. Brouwer and J. A. Ripmeester, *Crystal growth & design*, 2007, **7**, 1406-1410.
46. H. Moustafa, S. H. Shalaby, K. M. El-sawy and R. Hilal, *Spectrochimica Acta Part A: Molecular and Biomolecular Spectroscopy*, 2002, **58**, 2013-2027.
47. F. D'Amico, F. Bencivenga, G. Camisasca, A. Gessini, E. Principi, R. Cucini and C. Masciovecchio, *The Journal of Chemical Physics*, 2013, **139**, 015101.
48. F. D'Amico, F. Bencivenga, A. Gessini, E. Principi, R. Cucini and C. Masciovecchio, *The Journal of Physical Chemistry B*, 2012, **116**, 13219-13227.
49. M. Falk, M. Gil and N. Iza, *Canadian Journal of Chemistry*, 1990, **68**, 1293-1299.
50. M. G. Giorgini, *Pure Appl. Chem.*, 2004, **76**, 157–169.

51. G. Fini and P. Mirone, *J Chem Phys*, 1971, **71**, 2241.
52. G. Döge, R. Arndt and J. Yarwood, *Molecular Physics*, 1984, **52**, 399-414.
53. D. E. Logan, *Chemical Physics*, 1986, **103**, 215-225.
54. J. L. McHale, *The Journal of Chemical Physics*, 1981, **75**, 30-35.
55. D. E. Logan, *Molecular Physics*, 1986, **58**, 97-129.
56. C. W. Lehmann and F. Stowasser, *Chemistry – A European Journal*, 2007, **13**, 2908-2911.
57. J. Šponer, J. E. Šponer, A. Mládek, P. Jurečka, P. Banáš and M. Otyepka, *Biopolymers*, 2013, **99**, 978-988.